

A Ka-Band Full-360° Millimeter-Wave  
Reflective-Type Phase Shifter with  
Quadrature Hybrid Coupler

## Table of Contents

<i>Abstract</i> .....	4
<i>Introduction</i> .....	5
<i>Phase Shifter Theory</i> .....	6
<i>Ideal Phase Shifter</i> .....	6
<i>Design Specifications for Phase Shifters</i> .....	7
Frequency Capability and Bandwidth .....	7
Insertion and Return Losses .....	7
Linearity .....	8
Resolution and Phase Range .....	8
Power Handling .....	8
Amplitude and Phase Errors .....	8
Power Consumption.....	9
<i>Phase Shifter Topologies</i> .....	9
Switched Line Phase Shifter .....	9
High Pass - Low Pass Type Phase shifter .....	10
Loaded Transmission-Line Phase Shifter .....	12
Reflective-Type Phase Shifters.....	13
<i>28GHz RTPS Design Implementation</i> .....	15
<i>Topology Selection</i> .....	15
<i>Substrate Selection</i> .....	15
<i>Varactor Qualification and Analysis</i> .....	16
<i>Preliminary RTPS Design</i> .....	17
<i>Final RTPS Design</i> .....	18
Replacement of the lumped elements with transmission line stubs .....	20
Realization in Microstrip .....	21
<i>Future Improvement</i> .....	22
<i>Bibliography</i> .....	23

Figure 1: A radiating 5G MIMO array [3] .....	5
Figure 2: Phase vs frequency characteristics of constant phase type (left) and constant time delay shifter (right) .....	7
Figure 3: Switched Transmission Line Phase Shifter.....	10
Figure 4: Layout of Switched Transmission Line Phase Shifter [5].....	10
Figure 5: Low-pass pi (a), high-pass pi (b), low-pass T (c), high-pass T (d) networks .....	11
Figure 6: Switched High-Pass - Low Pass Pi phase shifter (left), Switched High-pass - Low-pass T phase shifter (right) .....	11
Figure 7: Transmission-Line Phase Shifter with shunt (a) and series (b) variable reactive loads.....	12
Figure 8: Simulation model of switched-line with loaded-line [7] .....	12
Figure 9: Reflective-Type Phase Shifter [8] .....	13
Figure 10: Simulated varactor capacitance over bias voltage range.....	16
Figure 11: A simple reflective phase shifter, using two varactor diodes .....	17
Figure 12: Phase range of the simple two-varactor design .....	17
Figure 13: The selected design of the full phase shifter, exposed as a two-port .....	18
Figure 14: Phase shift and gain of final RTPS design .....	19
Figure 15: S11 of the analysed system showing very low return loss.....	20
Figure 16: 2D view of the RTPS layout .....	21
Figure 17: 3D view of RTPS Layout.....	21

# Abstract

Phased array antennas are fundamental to modern radar and telecommunication systems, enabling electronic beam steering for applications ranging from military surveillance and weather monitoring to satellite broadband and emerging 5G/6G networks. Despite the numerous advantages of phased array systems with RF phase shift, including high signal-to-noise and signal-to-interference ratios, as well as low complexity, they present a few limitations, including high cost and large chip areas [1]. Their performance and cost, however, are heavily influenced by the design and efficiency of the RF phase shifters that control the relative phase between array elements. In this report, various electronic phase shifter architectures—namely switched-type, reflective-type, loaded-line, and high-pass/low-pass configurations—are discussed and evaluated for their suitability for high-frequency phased array implementations. Particular emphasis is placed on the design and realization of a 28 GHz reflective-type phase shifter implemented on a Rogers-based PCB substrate. The reflective-type topology is selected for its compact structure, continuous phase-tuning capability, and low power consumption. Design considerations including hybrid coupler selection, impedance matching, and reactive load implementation are discussed, and simulation results are analyzed to assess phase range, insertion loss, and return loss performance. The report demonstrates the potential of PCB-based reflective-type phase shifters as cost-effective and high-performance solutions for millimeter-wave phased array systems.

# Introduction

Antenna arrays have evolved dramatically since the introduction of the Yagi–Uda antenna in 1926 [2]. Early mechanically steered arrays gave way to solid-state electronic scanning with the advent of ferrite phase shifters in the 1950s. From the 1960s onward, phased-array systems (PAS) matured into compact, high-performance beamformers thanks to advances in antenna fabrication and integrated RF phase-shifter technologies. Modern PAS architectures exploit electronic beam-steering, enabling ultra-fast reconfiguration of main-lobes and nulls for enhanced signal-to-noise ratio (SNR) and signal-to-interference ratio (SIR). By precisely controlling the phase across each element, the radiation pattern can be shaped and steered dynamically across azimuth and elevation.

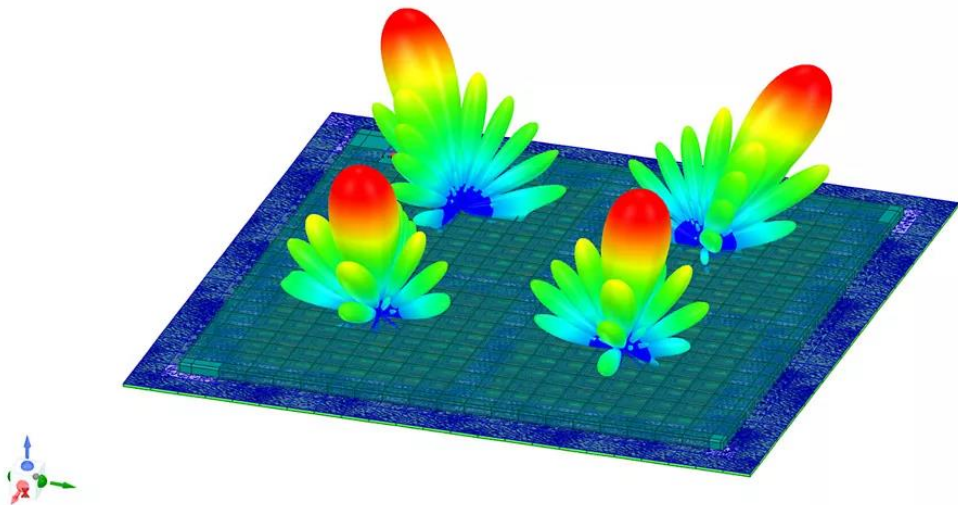


Figure 1: A radiating 5G MIMO array [3]

High-throughput satellite (HTS) ground terminals, high-mobility satellite-on-the-move (SOTM) systems, and next-generation 5G/6G millimeter wave communication all leverage PAS thanks to their ability to deliver massive spatial multiplexing, wide-angle scanning, and adaptive interference rejection. On the radar side, phased-array radars (PARs) support multi-object tracking, rapid volumetric scans, and degraded-grade resilience when one or more elements fail. Yet, despite their capabilities, phased arrays still face two critical bottlenecks: cost and footprint. While printed antennas are relatively inexpensive, the RF phase-shifters—responsible for steering the beam—often dominate the system's size, power budget and cost burden. At millimeter wave bands (e.g., 28 GHz), insertion loss, phase-resolution, tuning range and board real estate become even more critical.

# Phase Shifter Theory

## Ideal Phase Shifter

An ideal phase shifter can be defined through its scattering parameter matrix as:

$$S = \begin{bmatrix} 0 & Ae^{-j\phi} \\ Ae^{-j\phi} & 0 \end{bmatrix}$$

Where A is the gain of the phase shifter and  $\phi$  is the applied phase shift. The purpose of the phase shifter is to change the phase of the signal applied at its input in a known and well-defined manner. If  $\phi$  is constant, then the phase shifter is a Fixed Phase Shifter. If  $\phi$  can be varied through an external control signal, then the phase shifter is a Tunable Phase Shifter. Ideally, the gain of a tunable phase shifter remains constant when the phase shift varies. Nevertheless, based on the application, small variations of the gain can be tolerated [4].

Based on how the phase shift can be controlled, two major categories can be distinguished:

- Continuous phase shifters can vary the phase of the input signal in a certain range  $[\phi_{min}, \phi_{max}]$  in a continuous way. i.e. every phase within the range  $[\phi_{min}, \phi_{max}]$  can be obtained when the control voltages are set appropriately.
- Digital phase shifters can only apply certain phase shift values  $\phi_1, \phi_2, \phi_3 \dots \phi_n$  to the input signal. Usually, the phase shift is controlled by setting the corresponding control bits.

There are two other major phase shifter categories that are not immediately apparent from equation below. The equation can be modified so that it expresses the scattering parameter matrix over frequency:

$$S(\omega) = \begin{bmatrix} 0 & A(\omega)e^{-j\phi(\omega)} \\ A(\omega)e^{-j\phi(\omega)} & 0 \end{bmatrix}$$

As a result, based on the frequency variation of the phase shift, the following two categories could be specified:

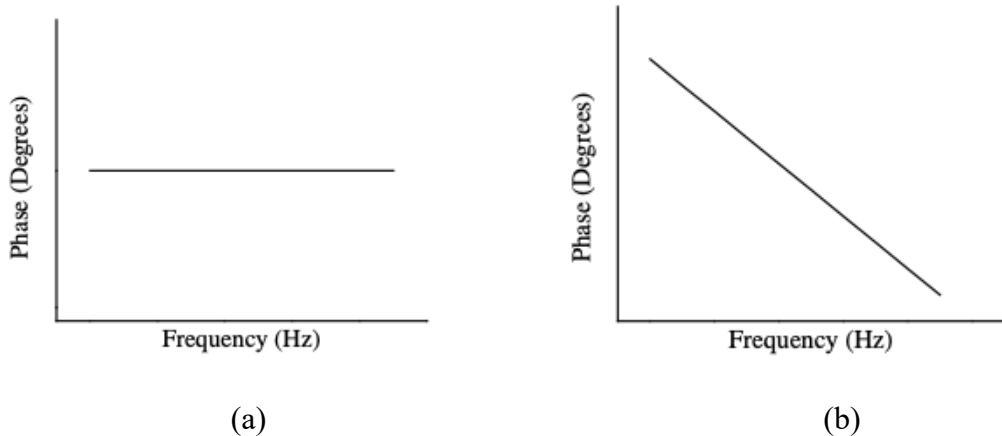


Figure 2: Phase vs frequency characteristics of constant phase type (left) and constant time delay shifter (right)

## Design Specifications for Phase Shifters

### Frequency Capability and Bandwidth

RF phase shifters are typically designed to operate at a center frequency  $f_0$  with a bandwidth  $BW = f_H - f_L$ , where  $f_H$  and  $f_L$  denote the upper and lower cutoff frequencies, respectively. While bandwidth is often defined as the 3-dB range, practical RF phase shifters may instead specify it as the frequency range where reflection coefficients ( $S_{11}$ ,  $S_{22}$ ) remain below  $-10$ dB. The fractional bandwidth (FBW), representing the normalized bandwidth, is expressed as  $FBW = (BW / f_0) \times 100\%$ . Achieving wideband operation at high frequencies is desirable but challenging, as the performance and quality factor of passive and active components deteriorate in the upper-GHz regime.

### Insertion and Return Losses

The insertion loss (IL) represents the energy loss of an RF phase shifter as the signal propagates from input to output and is defined as the negative of  $S_{21}$  in decibels.

$$IL = -20 \cdot \log|S_{21}|$$

The IL also indicates the phase shifter gain, and variations in gain across the operating bandwidth are referred to as gain imbalance, which should be minimized. Passive phase shifters generally exhibit higher insertion loss than active designs, and IL typically increases frequency. Conversely, the return loss (RL) quantifies the power reflected at the input or output ports. The input return loss is given by  $S_{11}$  and the output return loss by  $S_{22}$ :

$$RL_{in} = -20 \cdot \log|S_{11}|$$

$$RL_{out} = -20 \cdot \log|S_{22}|$$

For optimal performance, RF phase shifters should maintain low insertion loss and high return loss across the operating frequency band.

## Linearity

Linearity is a critical parameter in the design of RF phase shifters, ensuring that the output power varies linearly with the input power to minimize intermodulation distortion and facilitate accurate signal demodulation at the receiver. Like amplifiers, the linearity of an RF phase shifter is commonly characterized by its third-order intercept point (IP3), expressed as either the input (IIP3) or output (OIP3) intercept point. Passive phase shifters inherently exhibit higher linearity than active designs, as they lack active components that introduce non-linear behavior.

## Resolution and Phase Range

The phase range of a phase shifter is defined as the difference between the maximum achievable phase shift and the reference phase.

$$\Phi_{range} = \Phi_{max} - \Phi_{ref}$$

The resolution of a phase shifter represents the smallest phase increment between two consecutive phase states. This parameter is particularly relevant for digital or digitally controlled phase shifters and depends on the number of control bits  $N$ . It is given by:

$$\Phi_{res} = \frac{\Phi_{max}}{2^N}$$

For example, in a 2-bit phase shifter with a total phase range of  $\Phi_{max} = 360^\circ$ , the resolution is  $\Phi_{res} = 90^\circ$ , resulting in four possible phase states:  $\Phi_1 = 90^\circ$ ,  $\Phi_2 = 180^\circ$ ,  $\Phi_3 = 270^\circ$ , and  $\Phi_4 = 360^\circ$ . In practical implementations, digital phase shifters commonly exhibit a total phase range of  $360^\circ$  with resolutions up to 8 bits. While digital phase shifters provide discrete phase states, analog phase shifters offer effectively continuous resolution determined by the applied analog control voltage.

## Power Handling

RF phase shifters are often required to operate under high power levels while maintaining consistent performance. The power-handling capability is characterized by the one-dB compression point (P1dB), defined as the input (IP1dB) or output (OP1dB) power. Passive phase shifters typically exhibit superior power-handling capability compared to active designs, owing to the limited P1dB of transistors used in active circuits.

## Amplitude and Phase Errors

The phase error of an RF phase shifter represents the deviation between the desired and the actual measured phase shift, expressed as:

$$\Phi_{error} = \Phi - \Phi^0$$

Where  $\Phi$  is the measured phase and  $\Phi^0$  is the target phase. The root mean square (RMS) phase error is commonly used to quantify the overall accuracy of a phase shifter. For an  $N$ -bit digital phase shifter, the total number of possible phase states is  $M = 2^N$ . The RMS phase error is calculated as:

$$\Phi_{RMS} = \sqrt{\left[ \left( \frac{1}{M} \right) \cdot \sum_{n=1}^M (\Phi_n - \Phi_{0,n})^2 \right]}$$

Where  $\Phi_n$  and  $\Phi_{0,n}$  are the actual and target phase values for the  $n$ th state, respectively. Lower RMS phase error indicates higher phase accuracy and is particularly critical for digital phase shifters. The amplitude error represents the deviation between the theoretical and actual output amplitudes for a given phase state. In practice, both passive and active phase shifters typically exhibit amplitude errors below 3 dB, which are generally acceptable in phased array systems. Moreover, these errors can be mitigated using a variable-gain amplifier (VGA) or an attenuator following the phase shifter within the phased array system.

## Power Consumption

It is generally desirable for RF phase shifters to exhibit minimal or no DC power consumption, similar to other RF front-end components. However, many active phase shifters employ variable gain amplifiers (VGAs) for phase control, which results in notable DC power consumption. In addition, some architectures incorporate amplification stages to enhance output signal strength and linearity, further increasing power requirements. In contrast, digital phase shifters typically consume negligible DC power, as they primarily utilize passive components—such as inductors and capacitors—that do not draw continuous bias current or voltage.

## Phase Shifter Topologies

### Switched Line Phase Shifter

Switched-type phase shifters (STPS) are extensively employed in phased array systems due to their simplicity and robustness. The fundamental configuration of an STPS consists of two distinct signal paths with different electrical lengths, between which the input signal is alternately routed. This switching action is typically achieved using a single-pole double-throw (SPDT) switch controlled by a digital logic signal, rendering the STPS inherently digital in nature. The SPDT switches used in SLPS designs must exhibit high port-to-port isolation to ensure effective signal transmission and minimize leakage. Additionally, half-wavelength line sections should generally be avoided, as they can exacerbate return loss and degrade overall performance.

A specific implementation of the STPS is the switched-line (or switched-transmission-line) phase shifter (SLPS or STLPS). As shown in Figure 3, the SLPS comprises two transmission lines of unequal lengths.

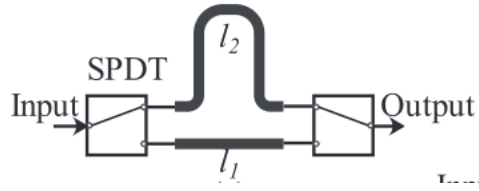


Figure 3: Switched Transmission Line Phase Shifter

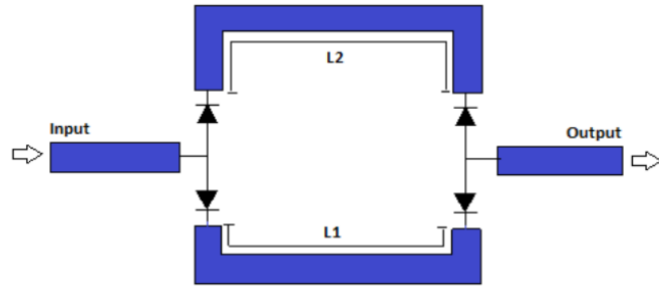


Figure 4: Layout of Switched Transmission<sup>i</sup> Line Phase Shifter [5]

Figure 4 illustrates the simplest version of SLPS, which uses four Single Pole Single Throw (SPST) switches to transmit signals between two transmission lines of varying lengths. The resulting phase shift between the two output states depends on the difference in line lengths and the signal wavelength, as expressed by:

$$\Delta\phi = \beta(l_1 - l_2)$$

Where  $l_1$  and  $l_2$  represent the lengths of the longer and shorter transmission lines, respectively, and  $\beta$  denotes the phase constant of the transmission medium. STPS structures offer several notable advantages, including low power consumption, high linearity, and substantial power-handling capability, owing to the absence of active components in the primary signal path. Nonetheless, their principal drawbacks include high insertion loss, limited switching speed, large chip area, and low phase resolution. To achieve wider phase coverage, multiple STPS units can be cascaded. The number of cascaded stages corresponds to the number of control bits of the phase shifter. Consequently, phase resolution increases with the number of bits, but this improvement comes at the expense of larger area and higher fabrication cost.

## High Pass - Low Pass Type Phase shifter

Pi and T-shaped networks as shown in Figure 5 can create a phase shift of  $-90^\circ < \Delta\phi < 90^\circ$  at a particular frequency  $\omega_o$  while remaining matched to  $Z_0$ . This smaller phase range necessitates cascading several of these networks.

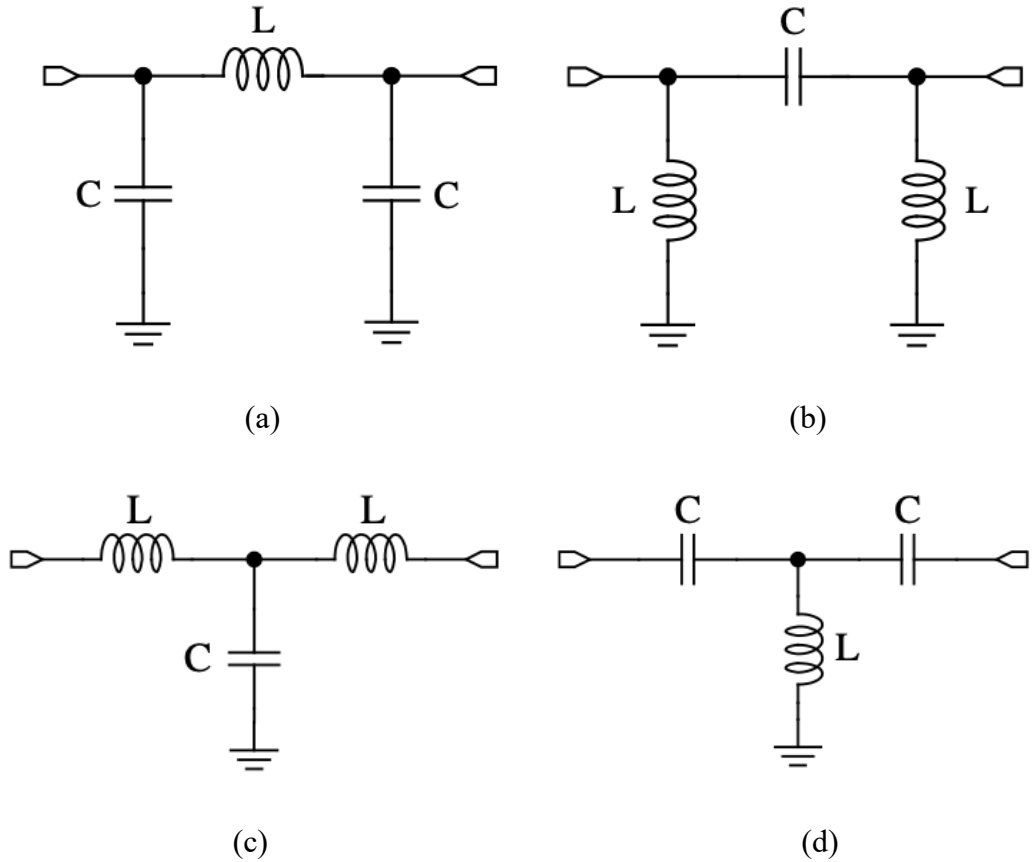


Figure 5: Low-pass pi (a), high-pass pi (b), low-pass T (c), high-pass T (d) networks

Two phase shifters that switch between a high-pass and a low-pass network are illustrated in Figure 6, resulting in a relative phase shift of  $0^\circ < \Delta\phi < 180^\circ$

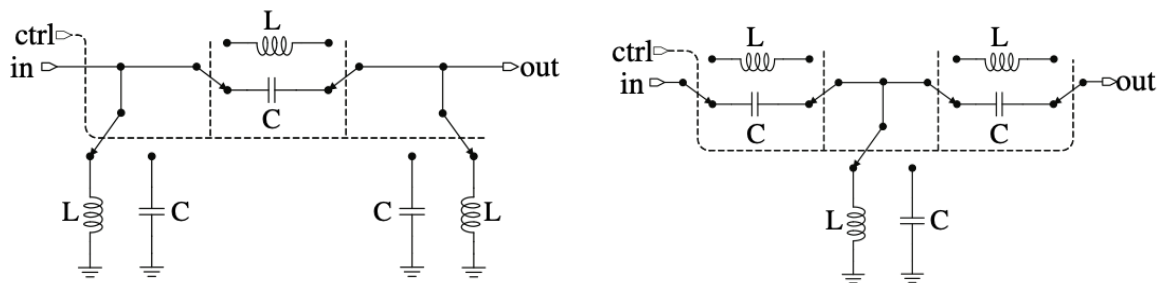


Figure 6: Switched High-Pass - Low Pass Pi phase shifter (left), Switched High-pass - Low-pass T phase shifter (right)

The high-pass – low-pass phase shifters can result in very compact size when realized in integrated circuit form with spiral inductors and MiM capacitors [6].

## Loaded Transmission-Line Phase Shifter

Loaded-line phase shifters (LLPS) are widely used in wireless communication systems to realize phase shifts typically less than  $180^\circ$ . A basic LLPS consists of a transmission line section combined with a series or shunt variable reactance, as illustrated in Figure 7.

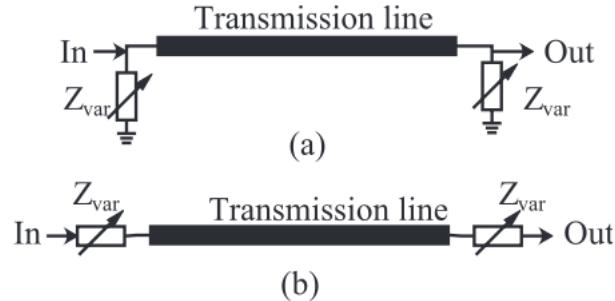


Figure 7: Transmission-Line Phase Shifter with shunt (a) and series (b) variable reactive loads

The variable reactance element can be either capacitive or inductive, and its tuning may be implemented in a continuous or discrete manner. Consequently, LLPS architectures can operate in either analog or digital modes. The loaded transmission line can be modeled as an equivalent line with an effective characteristic impedance and phase that vary with the load impedance  $Z_{var}$ . As a result, the effective impedance of the LLPS changes with phase tuning, which can lead to input and output impedance mismatches.

Figure 8 shows a simulation model combining a switched line and a loaded line. In this configuration, the longer path incorporates two tuning stubs—equivalent to loaded lines—positioned at each corner, whereas the shorter path includes a single stub located at its midpoint. Phase shift adjustment is achieved by modifying the lengths of these stubs.

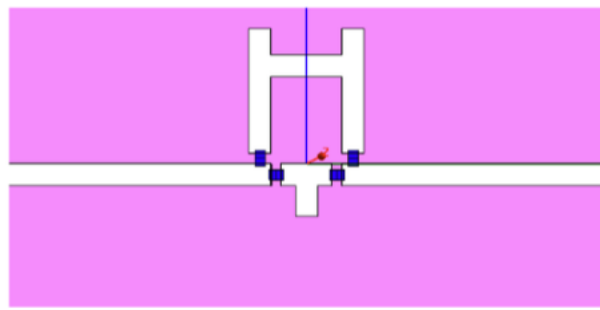


Figure 8: Simulation model of switched-line with loaded-line [7]

The principal limitations of LLPSs include poor return loss across different phase states and a restricted achievable phase range. The maximum phase range is primarily determined by the tunable load element, which is typically a varactor, while the transmission line length is commonly fixed at a quarter wavelength. An LLPS employing only varactor-based reactive loads can theoretically provide a maximum phase shift of approximately  $90^\circ$ .

## Reflective-Type Phase Shifters

The reflective-type phase shifter (RTPS) is widely employed in various applications, including phased array systems, due to its capability to provide precise and finely tunable phase shifts. The RTPS enables continuous phase control and is therefore categorized as an analog phase shifter, although digital-to-analog converters (DACs) may be used to discretize its control voltage.

A typical RTPS consists of a 3-dB hybrid coupler and two identical reflective loads connected to the through and coupled ports, as illustrated in Figure 9. The reflective loads are ideally purely reactive and are commonly realized using varactors, PIN diodes, or a combination of varactors and inductors. Depending on the coupler topology, the phase difference between its outputs may be  $90^\circ$  or  $180^\circ$ . Accordingly, branch-line and Lange couplers are frequently employed in RTPS implementations.

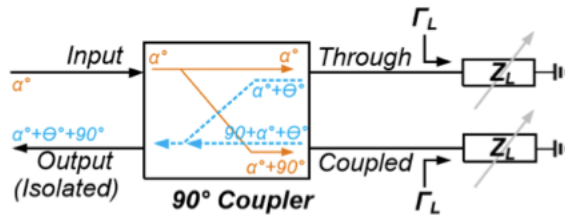


Figure 9: Reflective-Type Phase Shifter [8]

When an input signal is applied to the input port, it is divided equally by the hybrid coupler and reflected by the variable reactive loads at the through and coupled ports. The reflection coefficient of each load,  $\Gamma_{load}$ , is expressed as:

$$\Gamma_{load} = \frac{jX_{load}+R_0}{jX_{load}-R_0}$$

Where  $X_{load}$  represents the reactance of the variable load and  $R_0$  is the system's characteristic impedance. As evident from this relation, the phase of the reflected signal can be tuned by adjusting  $X_{load}$ .

The reflected waves from the through and coupled ports recombine within the hybrid coupler. At the input port, these reflected signals have a  $180^\circ$  phase difference and therefore cancel each other, while at the isolation port—serving as the output—they are in phase and add constructively. Consequently, the desired phase-shifted output is obtained at the isolation port. The overall phase shift range of an RTPS is given by:

$$\Delta\phi = 2[\tan^{-1}\left(\frac{X_{load,max}}{R_0}\right) - \tan^{-1}\left(\frac{X_{load,min}}{R_0}\right)]$$

Where  $X_{load,max}$  and  $X_{load,min}$  denote the maximum and minimum reactance values of the reflective load, respectively.

Theoretically, an ideal RTPS using purely reactive loads provides a phase range below  $180^\circ$ . However, practical implementations using diode-based tunable capacitors are further limited by their restricted capacitance variation, resulting in narrow tuning ranges. The phase range can be extended by employing composite reactive networks, such as varactor-inductor combinations. Parallel LC configurations generally yield broader phase ranges than their series counterparts. Another common technique to achieve a full  $360^\circ$  phase shift is cascading two quadrature couplers and employing  $\pi$ -type LC variable loads. Alternatively, transformer-based or multi-resonant variable loads can be utilized to achieve wideband  $360^\circ$  phase coverage at millimeter-wave frequencies.

The RTPS shares several advantages and limitations with the switched-line phase shifter, including low power consumption and good linearity. However, the inclusion of the hybrid coupler introduces additional insertion loss. The hybrid coupler, nonetheless, provides excellent port isolation and improved impedance matching, contributing to better overall signal integrity.

# 28GHz RTPS Design Implementation

## Topology Selection

The general principle of passive phase shifters requires either an inline transformer (such as in [9]) or a more traditional microwave way to implement coupling between lines. Since a transformer is difficult to implement at such a high frequency, the typical microwave coupling circuits are preferred. For a microstrip-based design, the leading options are a Lange coupler or a quadrature coupler.

Lange couplers can potentially reach as high coupling factors as quadrature couplers, but the ease of implementation in microstrip and very low reflections of the quadrature design make it a better choice for these applications. One notable consideration is bandwidth. While true that Lange couplers generally have higher bandwidth than quadrature couplers, the required bandwidth is application dependent. Frequency selectivity is often desirable, helping to filter out-of-band blockers and spurious interference.

## Substrate Selection

As is generally understood, FR4 is a poor substrate at microwave frequencies. High dissipation and losses result in poor coupling, lossy transmission, and behavior that is much further from the ideal components than is required. Rogers manufactures a wide variety of substrates suitable for higher frequencies. The Rogers High Frequency Product Selector Guide [10] suggests that TMM substrates would be suitable. These substrates have the low dissipation factors and the high relative permeability required to enable fabrication at these frequencies. Taking a middle-of-the-road substrate, such as the TMM6i, with an example thickness 1.524mm (matching what you might find in a 1.6mm FR4 PCB, for example), we can evaluate the required parameters of the microstrip transmission line:

Microstrip width: 1.69mm

Quarter-wavelength microstrip length: 1.13mm

Since the width is larger than the length, this design cannot be manufactured. The microstrip lines would overlap, and the coupler would function as a short circuit. Additionally, it is desired to have some safety margin between the thickness and length, to prevent the non-intentional capacitive coupling between the parallel traces. Since the microstrip length is relatively fixed (changing slightly over the range of relative permeabilities), we should try to reduce the trace width. To do this, we can use better and thinner substrates (higher permeability). Selecting the Rogers TMM 13i ( $\epsilon_r = 12.2$ ) substrate in the thinnest size listed (0.381mm), the ADS LineCalc tool suggests the following dimensions:

Microstrip width: 0.227mm

Quarter-wavelength microstrip length: 0.929mm

This design is clearly realistic, and so the TMM 13i substrate with a thickness of 0.381mm was selected.

## Varactor Qualification and Analysis

Although ideally a varactor would act as just a variable capacitor dependent on bias voltage, the parasitic losses and non-ideal properties cannot be neglected. Accordingly, a testbench was created in ADS per the manufacturer's datasheet [12], such to verify the capacitance as we sweep the bias voltage. The breakdown voltage of the MAVR varactor is 20V, which should be avoided with a suitable safety margin. Additionally, the varactor must not become forward biased. This results in a safe usable voltage range roughly of 1-15V. Analyzing the capacitance over this bias voltage range reveals a measured usable capacitance range of approximately 200fF – 800fF.

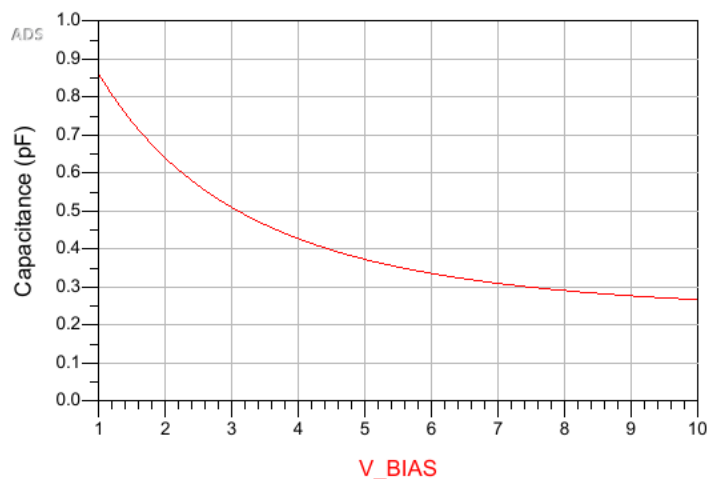


Figure 10: Simulated varactor capacitance over bias voltage range

## Preliminary RTPS Design

The most basic design phase shifter design uses two varactors and a common bias voltage. In this case, the maximum phase shift is gated by the ratio of the varactor capacitance over the accepted voltage range.

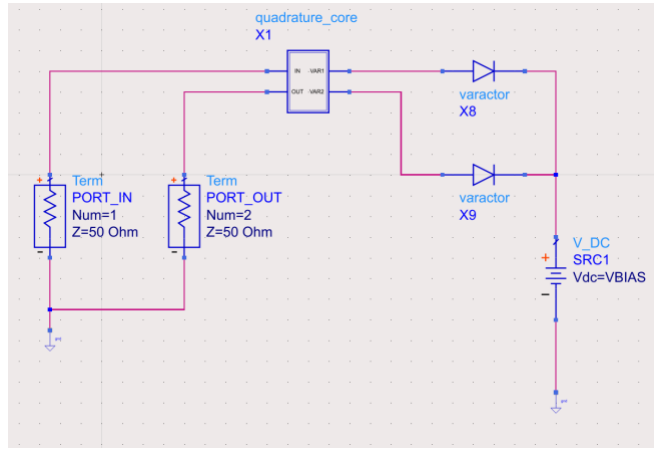


Figure 11: A simple reflective phase shifter, using two varactor diodes

Testing this phase shifter reveals that over the bias voltage range, a shift range of about 56 degrees is observed as in Figure 12.

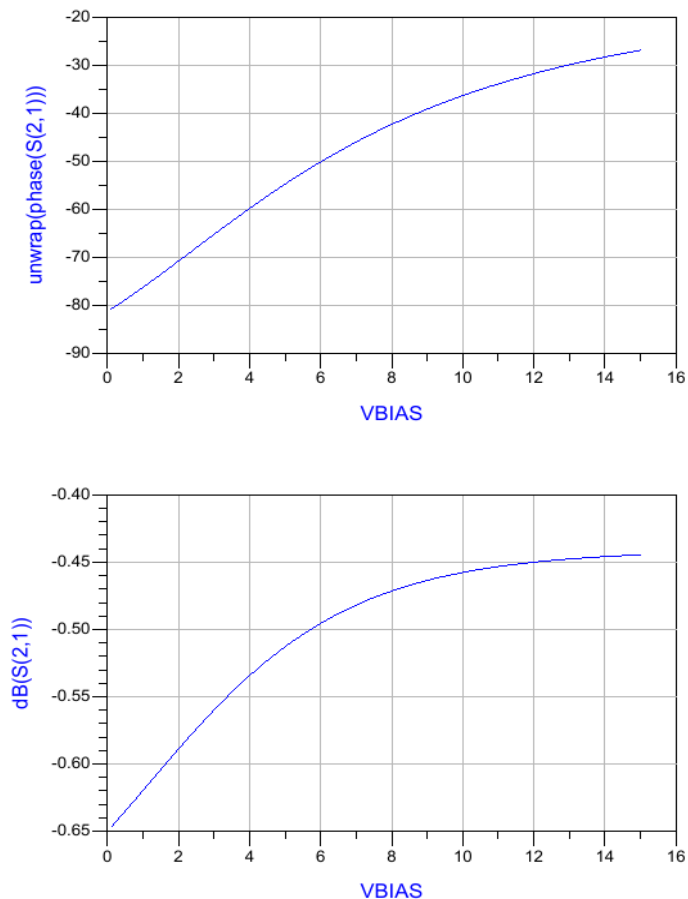


Figure 12: Phase range of the simple two-varactor design

## Final RTPS Design

Given the specification of a 360-degree shift, a more complex load than simply the varactor was required. Some notable load topologies were examined in [11], including a series LC load, dual matched LC loads tuned to resonance at the extremes (DRL loads), and the addition of a leading LC resonator to the DRL load to produce the “DRLT” topology [11]. As was shown in the referenced paper, the DRLT topology was most suited to the full-phase shift required.

The final design then can be seen in Figure 13:

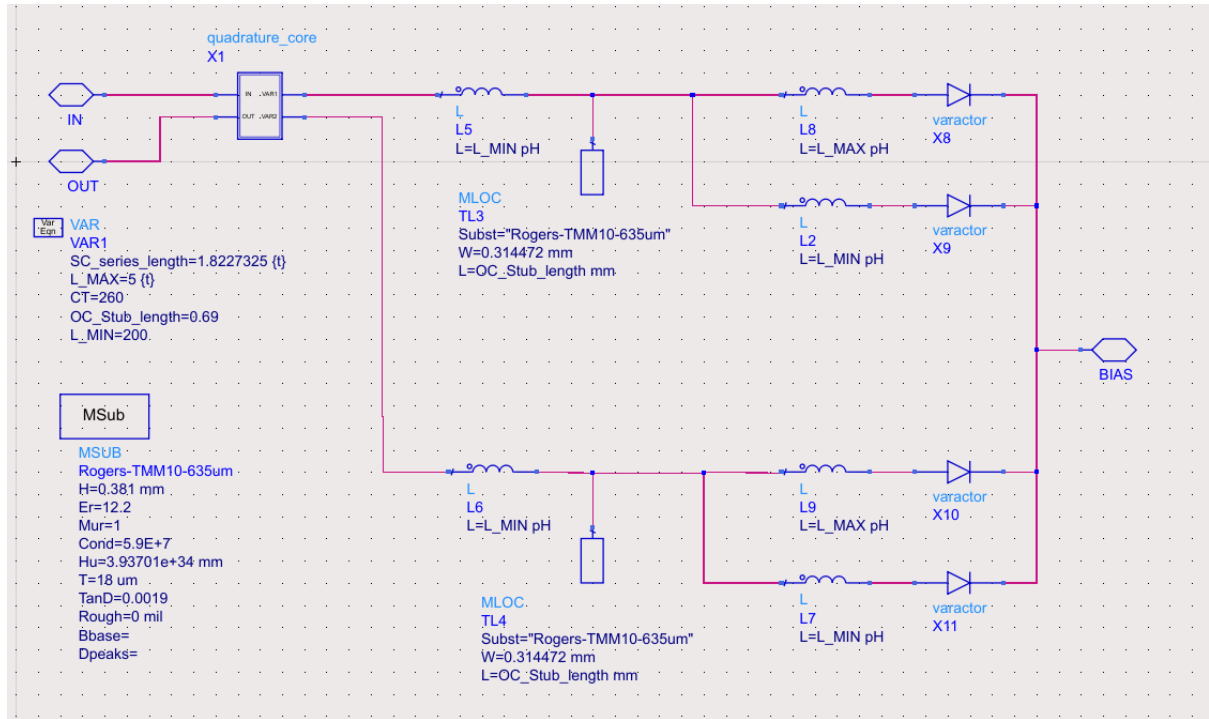


Figure 13: The selected design of the full phase shifter, exposed as a two-port

Analysis of the system showed monotonic performance, with the phase shift having a “S” shaped curve, as can be seen later in Figure 14. A “linear region” is observed, where the ratio of phase shift to bias voltage change is roughly constant. This curve shape and linear region is critical and influences how the design is optimized. Since the above referenced paper largely used ideal components, tuning is required to improve performance. To be able to tune the system, it was necessary to set some ideal output goals:

- The frequency shift should be monotonic – as the input voltage increases, the phase should always be increasing or decreasing as voltage increases. This makes it possible to use this type of phase shifter in circuits with negative feedback and analog control.
- $S_{21}$  should have as high a magnitude as possible. Although not a provided spec, it is undesirable to reflect energy back to the input or otherwise dissipate it in the circuit.

- The largest possible band of phase shift should be in the “linear region”. While not a hard quantifiable requirement, it would make the phase shifter easier to employ in practice. In general, the wider the “linear region” the lower the average slope of this region (degrees of phase shift per volt of bias) would be.
- In closed-loop operation, the lower gain will tend to make the system more stable when aiming for a DC phase shift.
- In open-loop operation with a look-up table, a very non-linear system would require an extremely high-voltage-resolution DAC to achieve a reasonable phase shift resolution.
- In open-loop operation without a look-up table, then only the phase shift available in the “linear region” would be usable.

In order to determine the desired values, the ADS tuning tool was employed, sweeping the  $L_{MIN}$  and  $L_{MAX}$  values to best achieve the design targets. Starting off with the suggested values, we can determine:

$$L_{max} = \frac{1}{\omega_0^2 * 200\text{pF}} = 161\text{fH}$$

$$L_{min} = \frac{1}{\omega_0^2 * 850\text{pF}} = 40\text{fH}$$

$$C_T = C_{MIN} = 200\text{pF}$$

$$L_T = L_{MIN} = 40\text{ fH}$$

Generally, tuning towards the criteria established above resulted in the values getting further apart, and the secondary LC tanks going “out of resonance”.

The selected values, which are near-optimal appear to be:

$$L_{MIN} = 5\text{ pH}$$

$$L_{MIN} = 200\text{ pH}$$

$$C_T = 260\text{ fF}$$

$$L_T = 200\text{ pH}$$

Simulating this circuit reveals the phase range and insertion loss of the system:

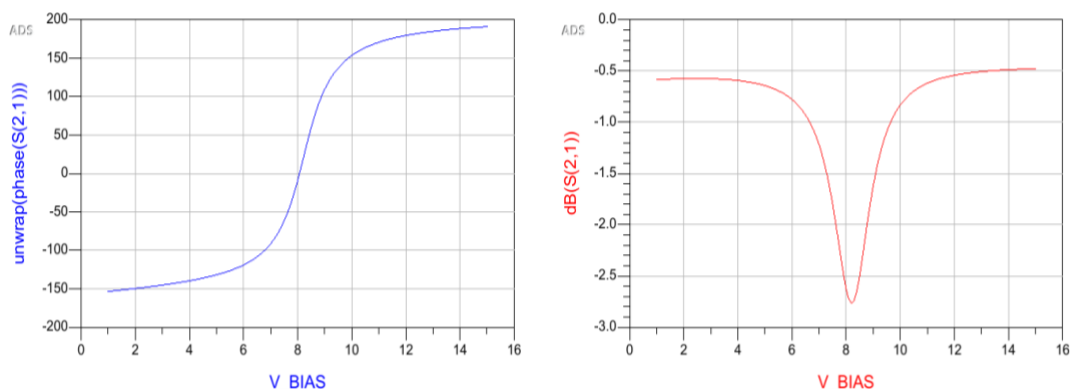


Figure 14: Phase shift and gain of final RTPS design

A phase shift of nearly 360 degrees (likely closer to 350) and insertion loss of <3dB is very close to or exceeding the specifications and goals.

In addition to the gain and phase shift, the return loss of the system can also be examined. An excellent input match is revealed, with at least 45dB of input. Although there is a significant difference at various bias voltages, the overall value is so low that reflections are basically irrelevant.

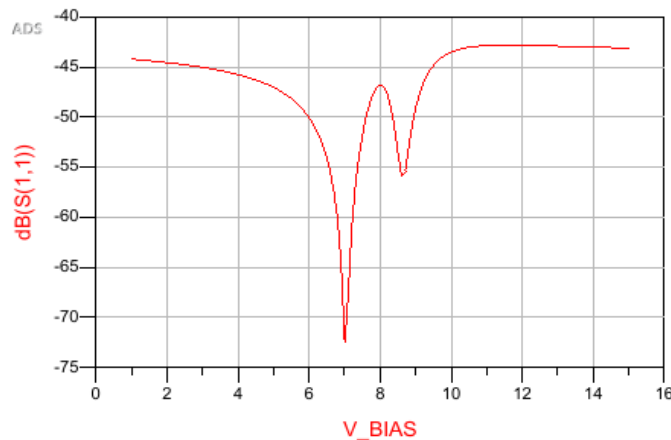


Figure 15: S11 of the analysed system showing very low return loss

## Replacement of the lumped elements with transmission line stubs

Finally, the capacitors can be replaced by open circuit parallel stubs. Applying the design equations for open circuit stubs, preliminary values can be determined:

$$l_s = 0.69 \text{ mm}$$

$$w_s = 0.31 \text{ mm}$$

Replacing the lumped inductors is very difficult due to the magnitudes involved and so was considered out of scope for this project. Accordingly, in addition to the four required varactors, this phase shifter also needs 4x 200pH inductors and 2x 5pH inductors as discrete components. These are available online as commodity items and best realized in 0201 packages to limit parasitic behaviours.

## Realization in Microstrip

The quadrature coupler was realized in the classical manner, as a microstrip box with parallel sides having different dimensions owing to the different characteristic impedances. The parallel capacitors were also realized as described above simply as open stubs. The lumped elements (inductors and varactors) were realized as 0201 packages as mentioned above. The final microstrip layout looks as follows:

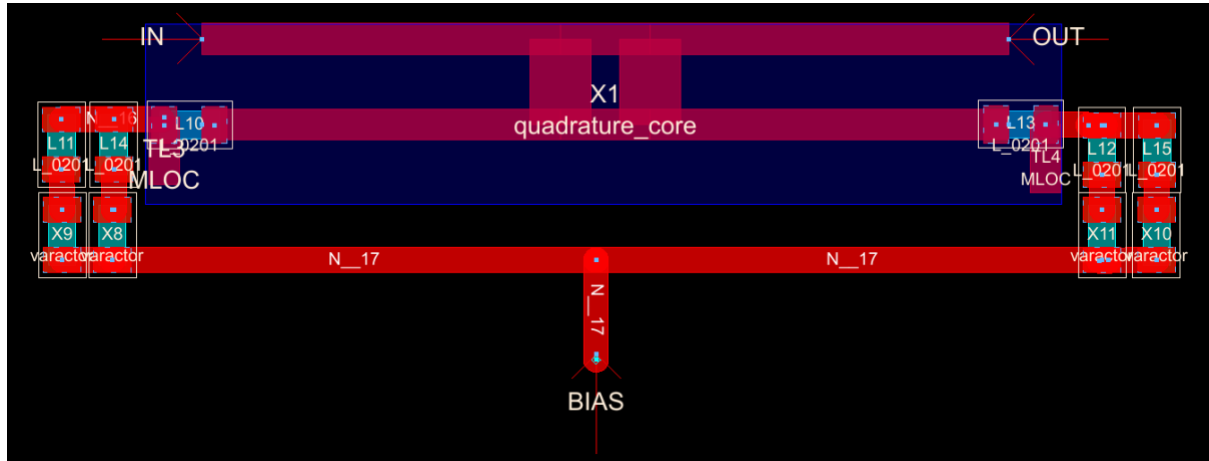


Figure 16: 2D view of the RTPS layout

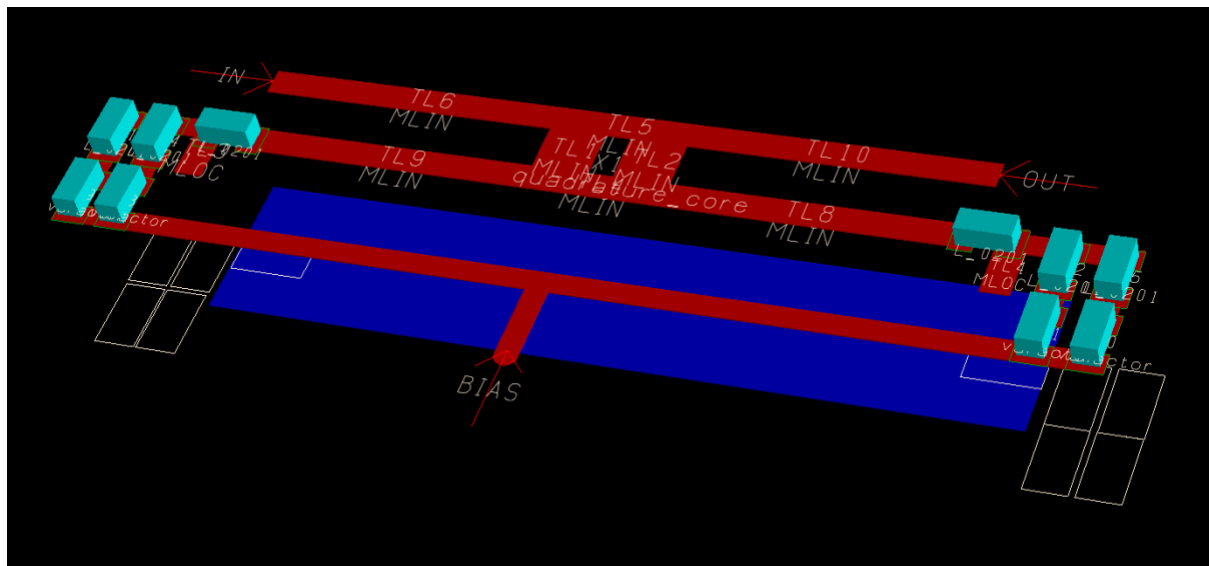


Figure 17: 3D view of RTPS Layout

## Future Improvement

This design was implemented using s-parameter analysis, using small signals. Once the input voltage range of the input increases above 2Vp-p, the diode will start to become forward biased. Subsequently, once it crosses 8Vp-p, the diode will see a peak voltage of 20V and may break down [12].

If this phase shifter were directly used to feed an antenna needing a high input voltage, for example, it may be worth using a smaller bias voltage swing centered around 8V or a similar value. Since the effective capacitance range between 5-11V of bias is dramatically much smaller than that of the 1-18V range, more varactors or a cascade-type system might be needed to achieve the 360 degrees of phase shift specification.

If larger bandwidth is required for some applications, it is likely worth investigating the use of a Lange coupler as opposed to a quadrature coupler hybrid. A Lange coupler will have higher bandwidth, with the trade-off of design complexity.

# Bibliography

- [1] Kebe, M., Yagoub, M.C.E. and Amaya, R.E. (2025), A Survey of Phase Shifters for Microwave Phased Array Systems. *Int J Circ Theor Appl*, 53: 3719-3739. <https://doi.org/10.1002/cta.4298>
- [2] H. Yagi, "Beam Transmission of Ultra- Short Waves," *Proceedings of the IRE* 16 (1928): 715–740.
- [3] Antenna gain explained: How to calculate and increase gain, <https://www.ansys.com/blog/calculate-and-increase-antenna-gain>
- [4] Gharsalli, S., Aloui, R., Mhatli, S., & Llamas-Garro, I. (2024). A Comprehensive Review on Phase Shifters:Topologies, Types, Comparative Studies, Liquid Metal Phase Shifters, and Future Directions. *Preprints*. <https://doi.org/10.20944/preprints202411.1386.v1>
- [5] Errifi, H.; Baghdad, A.; Badri, A.; Sahel, A. Electronically reconfigurable beam steering array antenna using switched line phase shifter. *2017 International Conference on Wireless Networks and Mobile Communications (WINCOM)*. IEEE, 2017, pp. 1–6.
- [6] I. Sarkas, "ANALYSIS AND DESIGN OF W-BAND PHASE SHIFTERS," 2010. [Online]. Available: [https://www.eecg.utoronto.ca/~sorinv/theses/Ioannis\\_Sarkas\\_MASc\\_thesis.pdf?utm\\_source=chatgpt.com](https://www.eecg.utoronto.ca/~sorinv/theses/Ioannis_Sarkas_MASc_thesis.pdf?utm_source=chatgpt.com)
- [7] Wang, Z.; Yan, B.; Xu, R.M.; Guo, Y. Design of a ku band six bit phase shifter using periodically loaded-line and switched-line with loaded-line. *Progress In Electromagnetics Research* 2007, 76, 369–379.
- [8] A. Basaligheh, P. Saffari, S. R. Boroujeni, I. Filanovsky, and K. Moez, "A 28–30 GHz CMOS Reflection-Type phase shifter with full 360° phase shift range," *IEEE Transactions on Circuits & Systems II Express Briefs*, vol. 67, no. 11, pp. 2452–2456, Jan. 2020, doi: 10.1109/TCSII.2020.2965395.
- [9] A. Basaligheh, P. Saffari, S. Rasti Boroujeni, I. Filanovsky and K. Moez, "A 28–30 GHz CMOS Reflection-Type Phase Shifter With Full 360° Phase Shift Range," in *IEEE Transactions on Circuits and Systems II: Express Briefs*, vol. 67, no. 11, pp. 2452-2456, Nov. 2020, doi: 10.1109/TCSII.2020.2965395
- [10] Rogers Corporation, "High Frequency Product Selector Guide." <https://www.rogerscorp.com/-/media/project/rogerscorp/documents/advanced-electronics-solutions/english/product-selection-guides/high-frequency-electronics-product-selector-guide.pdf> (accessed Nov. 25, 2025).
- [11] H. Zarei, C. T. Charles and D. J. Allstot, "Reflective-Type Phase Shifters for Multiple-Antenna Transceivers," in *IEEE Transactions on Circuits and Systems I: Regular Papers*, vol. 54, no. 8, pp. 1647-1656, Aug. 2007, doi: 10.1109/TCSI.2007.902440.

[12] Macom, “Solderable GaAs Constant Gamma Flip-Chip Varactor Diode.” Accessed: Nov. 25, 2025. [Online]. Available: <https://cdn.macom.com/datasheets/MAVR-000120-1411.pdf>

